MIT Libraries | DSpace@MIT

MIT Open Access Articles

Urban heat island mitigation in Singapore: Evaluation using WRF/multilayer urban canopy model and local climate zones

The MIT Faculty has made this article openly available. ***Please share*** how this access benefits you. Your story matters.

As Published: 10.1016/J.UCLIM.2020.100714

Publisher: Elsevier BV

Persistent URL: https://hdl.handle.net/1721.1/135289

Version: Author's final manuscript: final author's manuscript post peer review, without publisher's formatting or copy editing

Terms of use: Creative Commons Attribution-NonCommercial-NoDerivs License

Massachusetts Institute of Technology

Mughal et al, 2020. *Urban Climate*. DOI: 10.1016/j.uclim.2020.100714

Urban heat island mitigation in Singapore: evaluation using WRF/Multilayer Urban Canopy Model and local climate zones

M. O Mughal[1], Xian-Xiang Li[2,3,4,*] and Leslie K Norford[5]

[1]*CENSAM, Singapore-MIT Alliance for Research and Technology, Singapore*

[2]*School of Atmospheric Sciences, Sun Yat-sen University, Zhuhai, China*

[3]*Southern Marine Science and Engineering Guangdong Laboratory (Zhuhai), China*

[4]*Guangdong Province Key Laboratory for Climate Change and Natural Disaster Studies, Sun Yat-sen University, China*

[5]*Department of Architecture, Massachusetts Institute of Technology, Cambridge, Massachusetts, USA*

Submitted: July 3, 2020
Revised: August 26, 2020
Accepted: October 3, 2020

Article Highlights:

- UHI mitigation measures are evaluated using WRF and Local Climate Zone in Singapore
- Cool Roofs can reduce air temperature by 1.3 °C and thermal stress by 2-2.5 °C
- Higher thermostat temperature lowers AC emission by 20% and temperature by ~3 °C
- Air temperature would be ~1.4 °C higher by 2030, if Singapore is densified

[*]Corresponding author: Xian-Xiang Li, School of Atmospheric Sciences, Sun Yat-sen University, Zhuhai, Guangdong, China. Email: lixx98@mail.sysu.edu.cn

ABSTRACT

Mitigation and adaption measures must be designed strategically by urban planners, designers, and decision-makers to reduce urban heat island (UHI) related risks. We employed the Weather Research and Forecasting (WRF) model to assess UHI mitigation scenarios for the tropical city of Singapore during April 2016, including two heat wave periods. The local climate zones for Singapore were used as the land use/land cover data to account for the intra-urban variability. The simulations show that the canopy layer UHI intensity in Singapore can reach up to 5 ºC in compact areas during nighttime. The results reveal that city-scale deployment of cool roofs can provide an overall reduction of 1.3 ºC in the near-surface daytime air temperature in large low-rise areas. Increasing the thermostat set temperature to 25 ºC from 21 ºC in city-wide buildings can potentially reduce the air temperature due to less (~20%) waste heat discharge from air-conditioning units. A densification scenario considering an increase from approximately 7,000 people/km^2 (2016) to 9,000 people/km^2 (2030) under the current climate leads to air temperature increase of 1.4 ºC, which demonstrates the importance of limiting the densification of less compact areas in maintaining thermal comfort in the future.

Key words: Air-conditioning; city scale cool roof deployment; Tropical; Urban densification.

1. Introduction

Due to rapid urbanization and intensive infrastructure developments globally and regionally, many cities are suffering from the urban heat island (UHI) effect and its associated environmental and societal challenges. The UHI phenomenon refers to the increasing sub-surface, surface or air temperatures observed in an urban environment compared to those in its undeveloped rural surroundings (Chow and Roth, 2006). The UHI is generated in principle from reduced wind speed due to urban roughness, nighttime (daytime) longwave (shortwave) radiation trapping, building material thermal properties, the relative lack of vegetation and the anthropogenic heat released from human activities. Here our focus will be on the canopy layer UHI, which is defined as the difference of near-surface (2-m) air temperature between the urban and surrounding rural environments. The UHI phenomenon has been studied in various climate regions through either observation or numerical modeling in numerous studies (Mirzaei, 2015; Tzavali et al., 2015), which have helped improve our understanding of the characteristics and various factors responsible for UHI development (Roth and Chow, 2012). UHI can pose significant risk to human health and may increase morbidity (Phelan et al., 2015). Coastal, tropical and rapidly growing cities are especially susceptible to increasing temperatures (Li et al., 2016). The eventual impacts of UHI will be heightened if insufficient attention is paid to the deployment of effective mitigation strategies in these cities.

Various Numerical Weather Predictors (NWPs), downscaled to a resolution of 1 km, have been used to study UHI (Fallmann *et al.*, 2013, Li and Norford, 2016, Sharma *et al.*, 2017). An Urban Canopy Model (UCM) is needed within the NWP model to account for the effects of streets and buildings, including the single-layer (SLUCM) (Kusaka *et al.*,

2001) and multilayer (MLUCM) (Martilli, 2002) schemes. Ample urban canopy parameter (UCP) data, including land use/land cover (LULC) maps, building databases and satellite/LIDAR data, are needed to run UCMs but may not exist due to insufficient resources. An effort to create a global database of UCPs for urban climate studies is the World Urban Database and Access Portal Tools (WUDAPT). It comprises information on urban form and function that has been collected in a consistent manner and captures variations across the urbanized landscape (Ching et al., 2014). The WUDAPT database is structured into three levels and the base level of information (L0) consists of local climate zone (LCZ) map information. The LCZ classification was primarily designed to describe the impact of land use features on the local near-surface thermal environment, in particular the roles of land use and anthropogenic heat on the magnitude of the observed UHI. The LCZ map for Singapore was developed in Mughal et al. (2019), following the WUDAPT methodology (Ching et al., 2018) for level 0 data (Mills et al., 2015) and using Landsat 8 images and high-resolution building height data. This LCZ map is used in WRF/MLCUM in the present study to understand the intra-urban variability of UHI and responses to mitigation strategies in different LCZs.

Numerous mitigation measures can be adopted to reduce the impact of UHI (Leal Filho et al., 2017) including high reflective (cool) or vegetated (green) roofs, planting trees and vegetation, switching to cool paving materials or reducing the sky view factor (Zhou and Shepherd, 2010). One benefit of coupling urban schemes within mesoscale models is to evaluate and choose the best UHI mitigation strategies before actually implementing them (Masson, 2006). With advances in urban modelling, several mitigation strategies have been numerically tested, utilizing either SLUCM or MLUCM (Aflaki et al., 2017). The results

of the sensitivity studies by Li and Norford, (2016) revealed that the application of cool roofs at city scale could lead to the reduction of the near-surface air temperature and surface skin temperature during the daytime with negligible effects at night. A simulation of UHI mitigation strategies for New York City, which included increasing albedo through whitening roofs and other paved surfaces, revealed reductions of 0.7 ºC in air temperature (Phelan et al., 2015). Salamanca et al. (2012) studied the UHI pattern over Madrid and evaluated possible UHI mitigation measures. They showed that a high roof albedo contributes significantly to reducing the canopy layer UHI by 1–2 ºC. Fallmann (2014) showed that high albedo for buildings in Stuttgart reduces the maximum surface temperature by 3.5 °C and canopy layer UHI by about 2 °C.

Waste heat released from air-conditioning (AC) systems can increase the UHI intensity and air temperature (Ohashi et al., 2007; Wen and Lian, 2009; Salamanca et al., 2011,2012; De Munck et al., 2013). Increasing cooling demands of urban areas are likely to increase the local warming induced by expanding built-up environments and greenhouse-gas-induced global climate change (Georgescu et al., 2013). Kikegawa et al., (2003) showed that a mean air temperature reduction of 1.3 °C is achieved for a district in Tokyo, Japan, by removing waste heat generated by AC systems. Salamanca et al. (2014) reported a mean energy savings of 1277 MWh and ~1 ºC night-time cooling in the Phoenix metropolitan area (US), if the waste heat released from the AC systems is reduced to zero. Wang et al. (2018) found that water-cooled AC systems in Hong Kong could reduce the 2-m air temperature by around 0.5 – 0.8 °C during the daytime, and about 1.5 °C at 19:00–20:00. In Singapore, cooling demand due to ACs is almost 37% of the total electricity consumption in residential areas and 60% in office spaces (Chua et al., 2013) and in another

study, reported to be responsible for 40–50% of the total building electricity consumption in Singapore (Keung, 2010). Therefore, it is necessary to examine the electricity consumption due to ACs to sustainably meet future energy needs in rapidly urbanizing countries with hot and humid climates (Li, 2018), and it is interesting to estimate how the reduction of waste heat release impacts the air temperature and UHI in Singapore.

The percentage of global population in urban areas has been growing from its value of 34% in 1960, reaching 55.3% in 2018 and is projected to increase to 60.4% in 2030 (World Health Organization, 2018). The LULCs are rapidly changing with increasing global urban population. Consequently, surface roughness increases due to construction of buildings, evapotranspiration decreases by changing vegetated or natural surfaces to impervious surfaces, and the surface energy balance is modified by absorbing and reflecting solar radiation and discharging additional anthropogenic heat. These changes in turn lead to modifications of the planetary boundary layer (PBL) structure in and around urban areas by perturbing the wind, temperature, moisture, and turbulence (Miao et al., 2009). Therefore, the impacts of urban areas on the local and regional climates are important to understand in order to tackle the problems caused by urbanization and LULC changes. Chen et al. (2016) investigated the impacts of urbanization in Nanjing, East China using WRF and found that urban sprawl may increase the daily mean UHI intensity up to almost 0.74 ºC. Chen et al. (2014) found that under high urbanization scenarios, the Hangzhou (China) city center saw an average temperature increase of 0.74 ºC. González-Aparicio et al. (2014) showed that the UHI intensity could increase by 0.7 °C during summer in Bilbao, Spain if the city size were doubled with the same intensity of AH. However, if appropriate UHI mitigation measures are taken, the warming effect of future urban expansion and

densification can be rolled back (Georgescu et al., 2014). Despite the fact that the advancing line of urban settlements can be effectively traced in developing countries through remote sensing (Miller and Small, 2003), the data scarcity about urban morphology in these and under-developed countries demands the use of the LCZ technique to obtain a proxy to the actual urbanization pattern. Developing LCZ for the current urban settlements and relating them to future urban developments can give planners hints on such climate issues as the future increase in temperature and the UHI. In the present study we used these techniques with the current climate conditions; however, future work will use future climate trends and greenhouse gas emission scenarios to quantify the effect of climate change on urban temperature and UHI.

Most of the studies mentioned above were for mid-latitudes cities, although the situation in tropical cities may be different. The maximum UHI is generally lower in tropical cities and occurs earlier than in temperate regions (Chow and Roth, 2006). Moreover, it has been demonstrated that the drivers for UHI development vary in different cities (Zhao et al., 2014) and the effectiveness of UHI mitigation measures is also expected to depend on local conditions (Li and Bou-Zeid, 2014). Hence more investigations are required to evaluate the UHI mitigation measures in tropical cities with high building density such as Singapore. Our previous study (Mughal et al., 2019) investigated the UHI characteristics in Singapore using WRF/MLUCM and LCZs. The objectives of the present study are to further evaluate the impact of UHI mitigation strategies, including cool roof and indoor temperature set point, and of increased urban density, on near-surface air temperature and inhabitant heat stress in Singapore. The novelties of this study are 1) employment of LCZ in the UHI mitigation studies so that to demonstrate the different

mitigation effects in different LCZ areas; and (2) by considering the interaction of indoor and outdoor thermal environment, the impacts of anthropogenic activities are taken into account dynamically.

2. Experiments

2.1 Study area

Singapore is an island state located just north of equator, between 1º09' N to 1º29' N, and 103º36' E to 104º25' E. It has a typical equatorial wet climate, with the mean daily temperature minima in a range of 23–26 ºC and mean daily maxima between 31-34 ºC (Fong and Ng, 2012). The monthly mean temperature range is 26-27.7 ºC and the annual rainfall is ~2300 mm (Fong and Ng, 2012). The climate of Singapore is characterized by the Northeast and Southwest Monsoon seasons, separated by two short inter-monsoon periods. The Northeast monsoon season (December to March) comes with high monthly rainfall and stronger winds, and the Southwest monsoon (June to September) is a relatively drier period (Fong and Ng, 2012). Singapore's topography is mostly low-lying, undulating with a small range of hills at the center. The land area is currently 719 km^2 and is still increasing due to ongoing land reclamation projects (mostly along the southern coastline). The population of Singapore in June 2018 was 5,638,700, and is currently increasing at an average annual rate of 0.5% (Kim, 2018). The urban thermal environment is mostly affected by the changes in the landscape, i.e., urbanization and industrialization (Roth and Chow, 2012).

2.2 The WRF model setup, initialization and evaluation

This study utilizes a modified version of WRF model 3.8.1. The setup consists of five one-way nested domains (Fig. 1 a), with horizontal resolutions (grid numbers) of 24.3 (76x76), 8.1 (79x91), 2.7 (112x112), 0.9 (112x112), and 0.3 km (211x130). LCZ used as the LULC data for domain d05 (covering Singapore and part of Malaysia), is shown in Fig. 1b. There are 51 eta levels from the surface up to 50 hPa, with higher vertical resolution near the surface to better resolve the near-surface processes. A very hot period in April 2016 (with a mean monthly temperature of 29.4 °C, Singapore's second hottest month since 1929) coinciding with the development of a heat wave (Chew *et al.*, 2021) has been analyzed. The simulation begins at 0000 UTC 1 April and finishes at 0000 UTC 30 April (spin-up time included). The model is forced with initialization fields from the Global Data Assimilation System (GDAS) 6-hourly final analysis data on a 0.25º x 0.25º grid (National Centers for Environmental Prediction, National Weather Service, NOAA, 2015). Since regional models cannot resolve smaller spatial and temporal scales, unresolved physical processes are accounted for using physically based parameterization schemes. The NOAH (NCEP-Oregon State University-Air Force-Hydrology Lab) land surface model (LSM) (Chen and Dudhia, 2001) calculates surface sensible and latent heat fluxes and surface skin temperature and provides them as WRF's lower boundary conditions. The MLCUM model incorporating Building Effect Parametrization (BEP) and Building Energy Model (BEM) is used in the present study, where the fluxes for the impervious urban surface are provided by the BEP (Martilli, 2002) while the BEM (Salamanca and Martilli, 2010) calculates the buildings' anthropogenic heat based on the building energy balance. The BEP/BEM model simulates the energy exchanges between buildings and the surrounding atmosphere. The evolution of indoor air temperature and humidity is calculated separately for each floor of

Formatted: Fo

Deleted: 1

multi-story buildings. The model also considers natural ventilation, shortwave radiation penetrating through the windows and heat generated by the occupants and equipment. With the AC systems on, the indoor temperature is maintained at a fixed target value (the thermostat set-point temperature). Once this target is reached, the AC systems will extract all the extra sensible and latent heat and the corresponding heat associated with their electricity consumption.

Other physical parametrization schemes include Rapid Radiative Transfer long-wave radiation scheme (Mlawer et al., 1997), Dudhia shortwave radiation scheme (Dudhia, 1989), Bougeault and Lacarrere PBL scheme (Bougeault and Lacarrere, 1989), Monin-Obukhov surface layer scheme (Monin and Obukhov, 1954), Goddard microphysics scheme (Tao et al., 2016) and Kain-Fritsch cumulus scheme (Kain, 2004) (for the two outer domains only). The time step for this simulation was 81 sec for the domain d01, with a successive 3:1 ratio for the immediate child domain (i.e., the time step for the domain d05 is 1 sec).

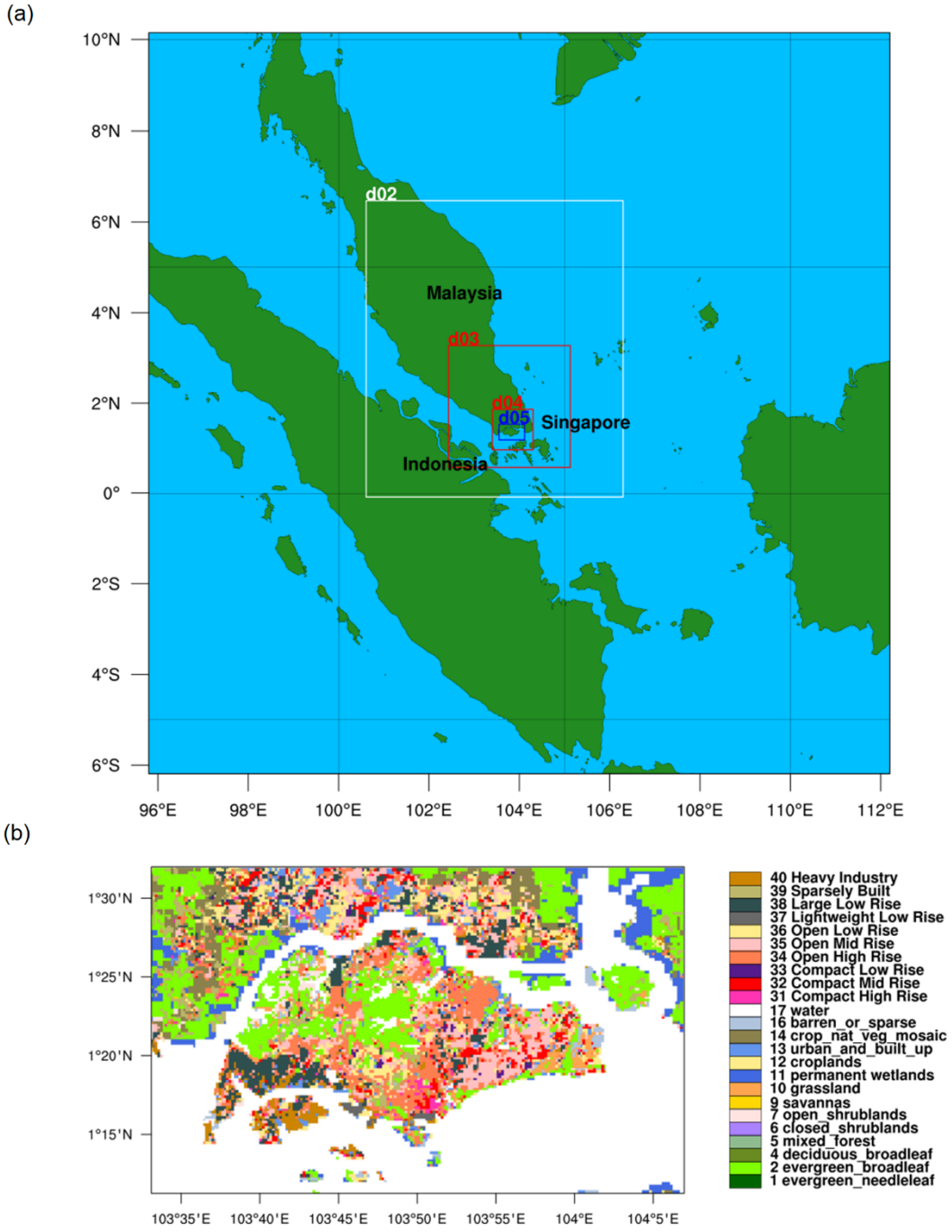

Fig. 1. (a) Configuration for WRF simulations (b) Land use/land cover map for domain d05 covering Singapore

The L0 data of the LCZ map for Singapore developed in Mughal et al. (2019) are incorporated into the WRF/MLUCM model using the method described in Martilli et al.

(2016) and are used as the LULC data for domain d05 (covering Singapore and part of Malaysia), as shown in Fig. 1 b. High cloud coverage over Singapore in LandSat 8 images was compensated using the *Mosaic* technique while the *Fmask* algorithm (Zhu et al., 2015; Qiu et al., 2017) was applied before mosaicking to further separate cirrus clouds, shadow, and water from clear pixels (Mughal et al., 2019). In the present study, the building height and the urban fraction values were obtained from high-resolution satellite data for Singapore. The width of the streets was approximated by considering the aspect ratio, the maximum height of the buildings per LCZ and their respective median values from Table 1 in Bechtel et al. (2015). Other urban parameters such as Roof-Road-Wall (RRW) surface albedo, RRW surface emissivity and RRW thermal conductivity were taken from Li et al. (2013). For want of data for different building types, the AC systems are assumed to be on for 24 hours a day with a set temperature of 21 ºC for all LCZs including both residential and commercial areas. It is further assumed that all heat emission from AC systems is rejected outdoors as sensible heat. Due to these considerations, the energy consumption provided must be considered only indicative. Nevertheless, the relative differences between the scenarios are probably a reliable indication.

Formatted: Fo

Deleted: 1

The WRF/MLUCM model has been evaluated in our previous study (Mughal et al., 2019) and was demonstrated to reproduce reasonably well the near-surface air temperature, relative humidity and solar radiation when compared with measurements from a sensor network across Singapore. Some of the comparisons and statistics from Mughal et al. (2019) are presented in the supplementary document for convenience. An index of agreement (IOA) of 0.97 for air temperature and 0.9 for the relative humidity was reported. In addition,

the global radiation component from the model compared favorably (IOA 0.92) with the observed values from five different measurement stations.

2.3 UHI and mitigation strategy assessment methods

2.3.1 UHI methodology

The model configuration described in section 2.2 will be termed hereafter as the Control case. Because UHI is the difference between the urban and rural air temperature and pure rural sites (no human intervention and no urban development in past years) are almost nonexistent in Singapore, an alternative scientific approach is to hypothesize a scenario that replaces the current urban areas with dense forest. This hypothesized scenario will be termed hereafter as "AllGreen." The model configuration of the Control and AllGreen cases is exactly the same except for the LULC. The UHI intensity is calculated as the 2-m temperature difference between the Control and AllGreen (or between densification and AllGreenMod) cases. This way the effects of sea breezes, cloud and topography can be avoided (Bohnenstengel et al., 2011). All the analyses will be based on the results for domain d05. A masking technique was applied to filter out the part of Malaysia in domain d05 and therefore the UHI intensity is only for Singapore.

2.3.2 Cool roof

The configurations for the WRF model for evaluating this mitigation strategy have been kept the same as those of the Control experiment, except that in the MLUCM the cool roof is implemented by changing the roof albedo from 0.2 to 0.86 in increments of 0.2. Three experiments have been performed in total, using albedo values of 0.4, 0.6 and 0.86.

The value of 0.86 was selected from the EPA Energy Star SOLARFLECT coating[1] to evaluate an extreme case of high albedo material. Cool white coatings (Pisello, 2017), which are typically elastomeric or cementitious, have solar reflectance values ranging from 0.7 to 0.85; therefore 0.86 can be considered an extreme value but still reasonable in terms of applicability. The main focus was to evaluate the thermal difference between a current albedo scenario (0.2) and a hypothetical scenario with albedo of 0.86. The incremental increase in the values of the reflectivity helped determine the intermediate changes in the temperature. The intermediate values of reflectivity were also derived from EPA Energy Star.

The level of thermal stress alleviated by increasing the albedo was analyzed by evaluating the Heat Index (*HI*). The *HI* combines temperature and relative humidity and was developed as a heat stress early warning system for the United States National Weather Service (NWS) (Buzan et al., 2015). The index was developed as a polynomial fit to Steadman's (1979) comfort model (Rothfusz, 1990). Here a definition in degrees Celsius is used rather than degrees Fahrenheit (Fischer and Schär, 2010):

$$HI = c_1 + c_2T + c_3T^2 + RH(c_4 + c_5T + c_3T^2) + RH^2(c_7 + c_8T + c_9T^2), \quad (1)$$

where air temperature (T) and *HI* are in °C, *RH* is the simultaneous relative humidity in percent and the coefficients $c_1 = -8.7847$, $c_2 = 1.6114$, $c_3 = -0.012308$, $c_4 = 2.3385$, $c_5 = 0.14612$, $c_5 = 2.2117 \times 10^{-3}$, $c_7 = -0.016425$, $c_8 = 7.2546 \times 10^{-4}$, and $c_9 = 3.582 \times 10^{-6}$. Some adjustments (Rothfusz, 1990) need to be made in some ranges of T and *RH*. Eq. *(1)* has a number of assumptions: the subject is a 67 kg male who is walking in shorts

[1] http://coolroofs.org/products/results/search&channel=products&orderby=cf_product_manufacturer+cf_product_brand+cf_product_model+asc&cf_product_init_solar_refl-from=0.86/P50

and a T-shirt (Rothfusz, 1990), and not in direct sunlight. *HI* uses a scale for determining heat stress: 26.6–32.2 °C is caution, 32.7–39.4 °C is extreme caution, 40–51.1 °C is danger, and ≥ 51.6 °C is extreme danger.

2.3.3 Indoor thermostat set temperature

To quantify the impact of AH from AC systems on Singapore's UHI and air temperature, two tests were conducted by 1) running the model without anthropogenic heat, which will be termed "NoAH;" and 2) running it with increased thermostat indoor temperature which will be termed as "ITIT." Generally, AC systems cool the indoor air by removing heat from the building interiors and release heat into the outdoor environment. The heat expelled from these systems outdoors is greater than the heat that must be removed to maintain the indoor temperature constant. As a consequence, the outdoor temperature is increased, and the cooling demand increases the electricity consumption. The thermostat setting in most office buildings in Singapore is 21 ºC (Damiati et al., 2015), which creates very high cooling demand. Therefore, a mitigation strategy is proposed to increase the indoor thermostat set temperature to 25 ºC (the ITIT case) and the effect will be evaluated here. These fluxes were evaluated for the Control and ITIT cases. In the NoAH case, there is no indoor target temperature, and the indoor temperature is determined based on the outdoor temperature and heat transfer through walls.

2.3.4 Urban densification

An urban densification scenario is studied to demonstrate how UHI will be deteriorated when Singapore is densified in the future. The change in UHI due to urban densification is determined by 1) replacing the LULC in the Control case with a future urban classification based on the Singapore's 2014 master plan, which will be termed the densification scenario;

and 2) adding reclaimed areas to the LULC data and replacing the urban areas with forest, in a scenario termed AllGreenMod. The parameters for each LCZ in the densification scenario are kept the same as those in the control case, and future climate change is not considered. It should be noted that this study considered the heat stored in the buildings due to radiation absorption, the heat trapping in the urban canyon and the contribution of the waste heat released from AC systems, but not the heat emissions from industrial processes.

3. Results

3.1 UHI characteristics

Our previous study (Mughal et al. 2019) demonstrated that during most of the night, i.e. from 21:00 LT to 04:00 LT, the UHI intensities are smooth and stay at their daily peak between 2.2 and 3.6 ºC for all the LCZs. The spatial distribution of the ensemble UHI intensity shows that higher UHI intensities are associated with urban areas, especially the commercial areas in southern Singapore. The night-time UHI intensity was much higher (~2°C) compared to Li et al. (2013), with a maximum of 4.2 ºC near the city center, while the daytime UHI intensity was quite small (~1°C).

3.2 Evaluation of UHI mitigation strategies

3.2.1 City wide impact of cool roof

Cool roofs refer to those roofs in an urban fabric with high surface reflectance (or albedo). They absorb less incoming radiation and have lower temperature compared to surfaces with lower surface reflectance, if all other conditions are equal. Cool roofs are generally proposed as a strategy to counter the UHI effect, and improve the outdoor air

quality and thermal comfort by reducing the cooling energy usage in air-conditioned buildings and increasing thermal comfort in unconditioned buildings in warm regions. Given the high density of Singapore's urban area, cool roofs have a large potential for passive cooling.

The spatial and temporal average 2-m temperature differences between the Control case (albedo value 0.2) and Cool roof cases (with albedo ranging from 0.4 to 0.86) for each LCZ class are shown in Fig. 2. The cool roof deployment with albedo 0.86 in the Large Low Rise (LCZ 8) area (Fig. 2h) can reduce the near-surface air temperature by 1.3 ºC at 13:00 LT. However, the cool roof deployment can only reduce the near surface air temperature in the same areas during nighttime by about 0.1 ºC. Comparably higher cooling effects in LCZ 8 were observed than those in the other areas due to its higher building density. The UHI intensities for each of the LCZ areas at 13:00 LT are shown in Table 1, and it is clear that for each LCZ, the increase of albedo leads to a reduction in UHI intensity during noon time. Comparatively more cool islands (negative values) exist in more LCZ classes for albedo 0.86. No cool islands are observed in case of albedo 0.2, while albedos 0.4 and 0.6 produce cool islands for LCZ9 (Sparsely Built Area) and LCZ 7 (Light Weight Low Rise), respectively. Fig. 3 shows the spatial distribution of temperature between the Control and the albedo cases of 0.4, 0.6 and 0.86, respectively for 14:00 LT and 21:00 LT. It is clearly seen that the effect of increasing albedo is much more significant during the day than at night.

Deleted: 2
Formatted: Fo
Deleted: 2
Formatted: Fo
Formatted: Fo
Deleted: 1
Deleted: 3
Formatted: Fo

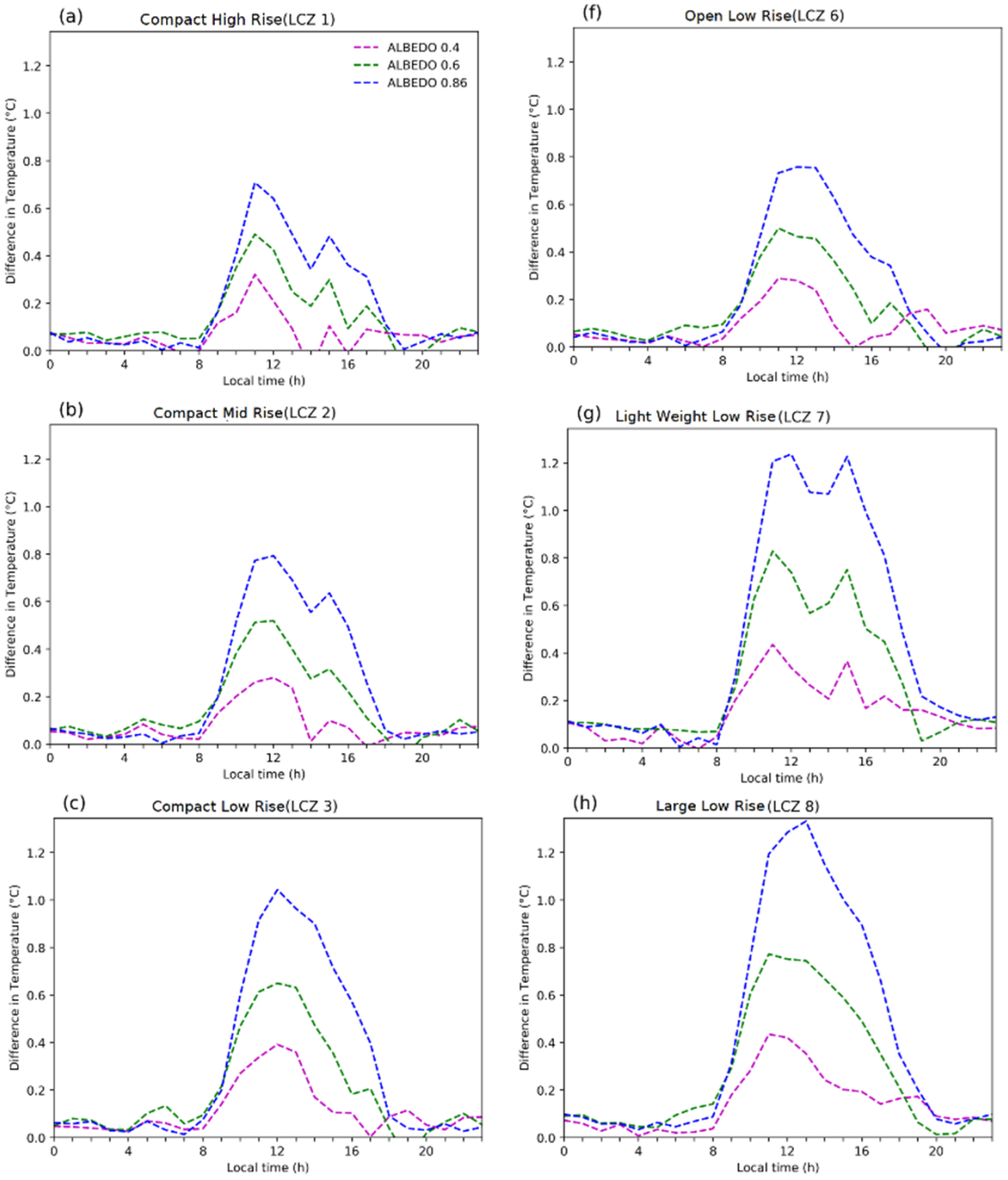
(a)
Compact High Rise(LCZ 1)
ALBEDO 0.4
ALBEDO 0.6
ALBEDO 0.86
(b)
Compact Mid Rise(LCZ 2)
(c)
Compact Low Rise(LCZ 3)
(f)
Open Low Rise(LCZ 6)
(g)
Light Weight Low Rise(LCZ 7)
(h)
Large Low Rise(LCZ 8)
Difference in Temperature (°C)
Local time (h)

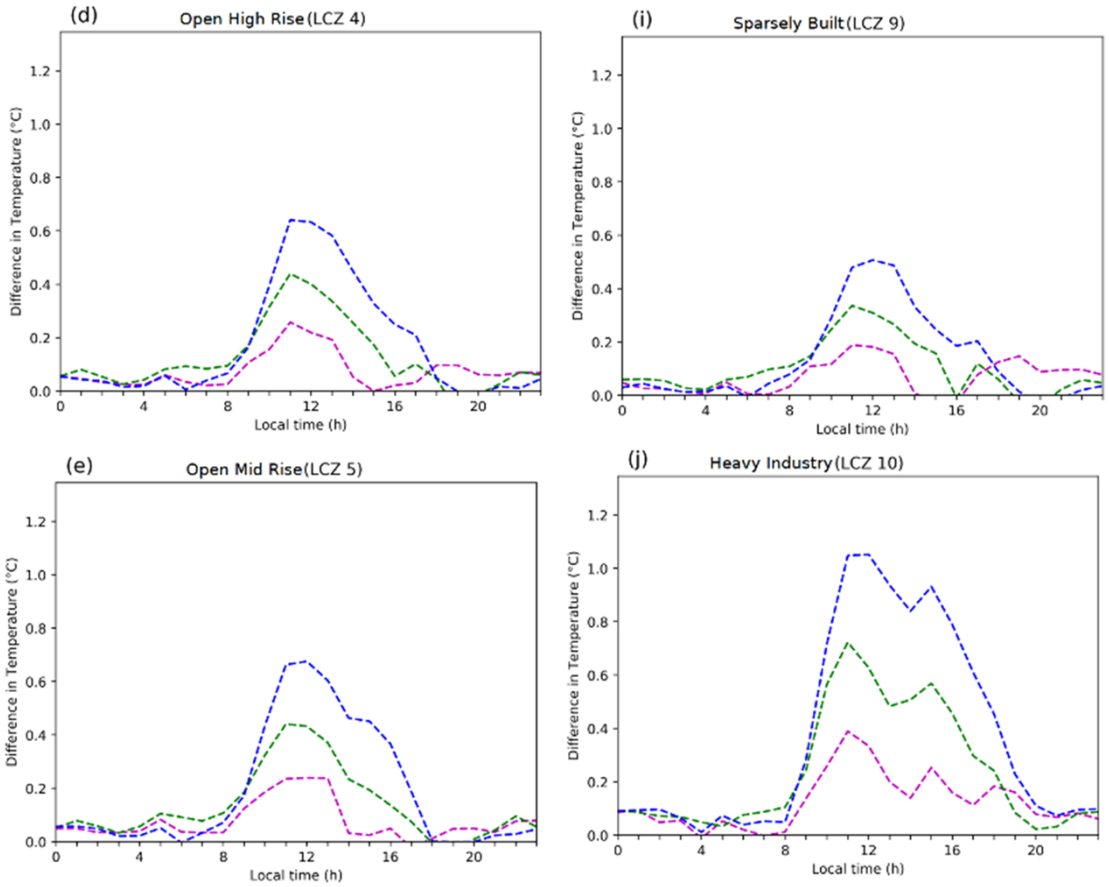

Fig. 2 Ensemble-averaged difference in 2-m temperature for April 2016 between the Control and Cool roof cases for each LCZ class.

Table 1 The UHI intensity for Albedo values ranging from 0.2 to 0.86 at 13:00 LT

	UHI intensity (ºC) at 13:00 LT			
LCZ Class	**Albedo 0.2**	**Albedo 0.4**	**Albedo 0.6**	**Albedo 0.86**
Compact High Rise (LCZ 1)	1.7	1.5	1.4	1.2
Compact Mid Rise (LCZ 2	1.4	1.1	1	0.7
Compact Low Rise (LCZ 3)	1	0.7	0.4	0.1
Open High Rise (LCZ 4)	1.2	1.1	0.9	0.7
Open Mid Rise (LCZ 5)	0.9	0.7	0.5	0.3
Open Low Rise (LCZ6)	0.6	0.5	0.2	-0.001
Light Weight Low Rise (LCZ 7)	0.4	0.18	-0.1	-0.6
Large Low Rise (LCZ 8)	1.4	1	0.7	0.1
Sparsely Built (LCZ 9)	0.04	-0.06	-0.1	-0.3
Heavy Industry (LCZ 10)	1.26	1.07	0.7	0.3

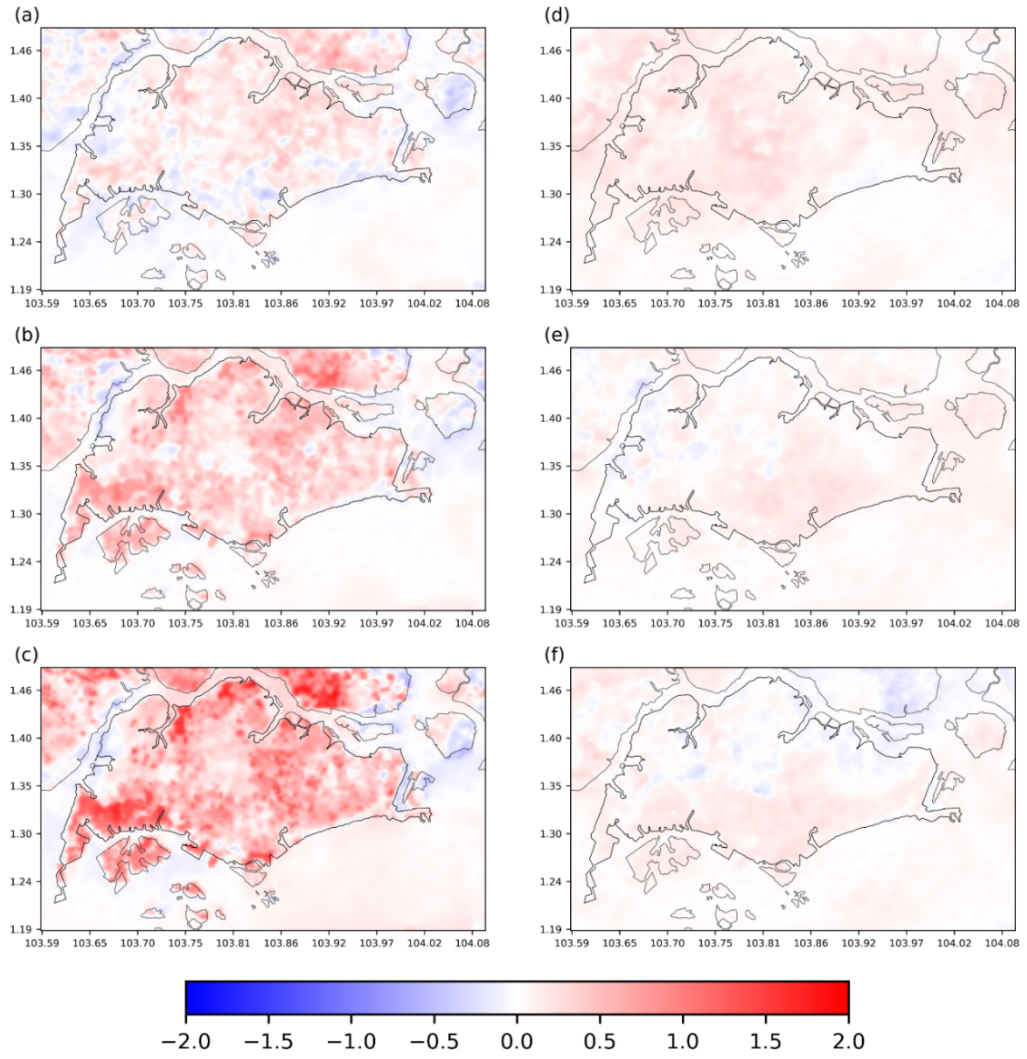

Fig. 3 Spatial temperature change at 14:00 LT (left) and 21:00 LT (right) between Control case and cool roof cases with albedo values of 0.4 (a, d), 0.6 (b, e) and 0.86 (c, f).

To better understand the mechanisms driving the temperature change, the surface energy balance will be examined:

$$Q^* + Q_F = Q_H + Q_E + \Delta Q_S, \quad (2)$$

where Q^* is the net all-wave radiation, Q_H and Q_E are the turbulent sensible and latent heat fluxes, ΔQ_s is the net storage flux, and Q_F is the anthropogenic heat flux. Q^* includes four components:

$$Q^* = S\downarrow(1-\alpha) + L\downarrow - L\uparrow, \quad (3)$$

where $S\downarrow$ is the incoming shortwave radiation, α is the albedo, and $L\downarrow$ and $L\uparrow$ are incoming and outgoing longwave radiation, respectively.

The energy balance and energy balance difference compared to that in the Control case (albedo value 0.2) for each albedo value are shown in Fig. 4. The highest difference in the net radiation and sensible heat flux existed for albedo value of 0.86 at 13:00 LT. Increasing the albedo value in Eq. *(2)* reduced the net shortwave radiation, thus decreasing the net all-wave radiation. Q_H is almost halved during daytime, causing a reduction in air temperature. It is noteworthy that the reductions of Q^* are nearly the same as those of Q_H irrespective of the roof albedo increase, suggesting that the latter is possibly caused by the former. Although there was no evapotranspiration on the cool roof, the increase in albedo still reduced the latent heat flux over the urban surface. Close inspection revealed that this reduction in the latent heat flux occurred over the vegetated part of the urban surface, where the reduced Q^* resulted in lower evapotranspiration. This is an interesting indirect effect related to city-scale changes in ambient air, which was also reported by Li and Norford, (2016). During nighttime both Q_H and Q_E remained close to zero due to the absence of shortwave radiation. By increasing the albedo to 0.86, the overall Q_F from AC systems was decreased by 6.7 Wm^{-2} at 16:00 LT, confirming less cooling load demand. However, this reduction was quite low as the outdoor air temperature reduction was generally below 1 ºC. ΔQ_s decreased significantly during daytime as the albedo increased. These storage fluxes

Formatted: Fo
Deleted: 4

are usually either stored in the roof, walls or ground and later released, or conducted into the indoor space and then typically pumped back outdoors by ACs. Thus, by considerably lowering ΔQ_s, the cool roofs can lower cooling loads and reduce anthropogenic heat releases, including the heat pumped back outdoor by ACs. Cool roofs with a maximum value of albedo can reduce the total electricity consumption by ~627 MW island-wide (Fig. S8) at 17:00 LT with a maximum reduction of 175 MW obtained in LCZ 4 at 17:00 LT. During nighttime, ΔQ_s was negative (meaning the heat flow is from the building interior towards the roof–air interface), and the positive differences of ΔQ_s for cool roofs indicate that less heat flowed towards the roof–air interface with increasing value of albedo. This resulted from the lower storage of heat during daytime in the cool roofs.

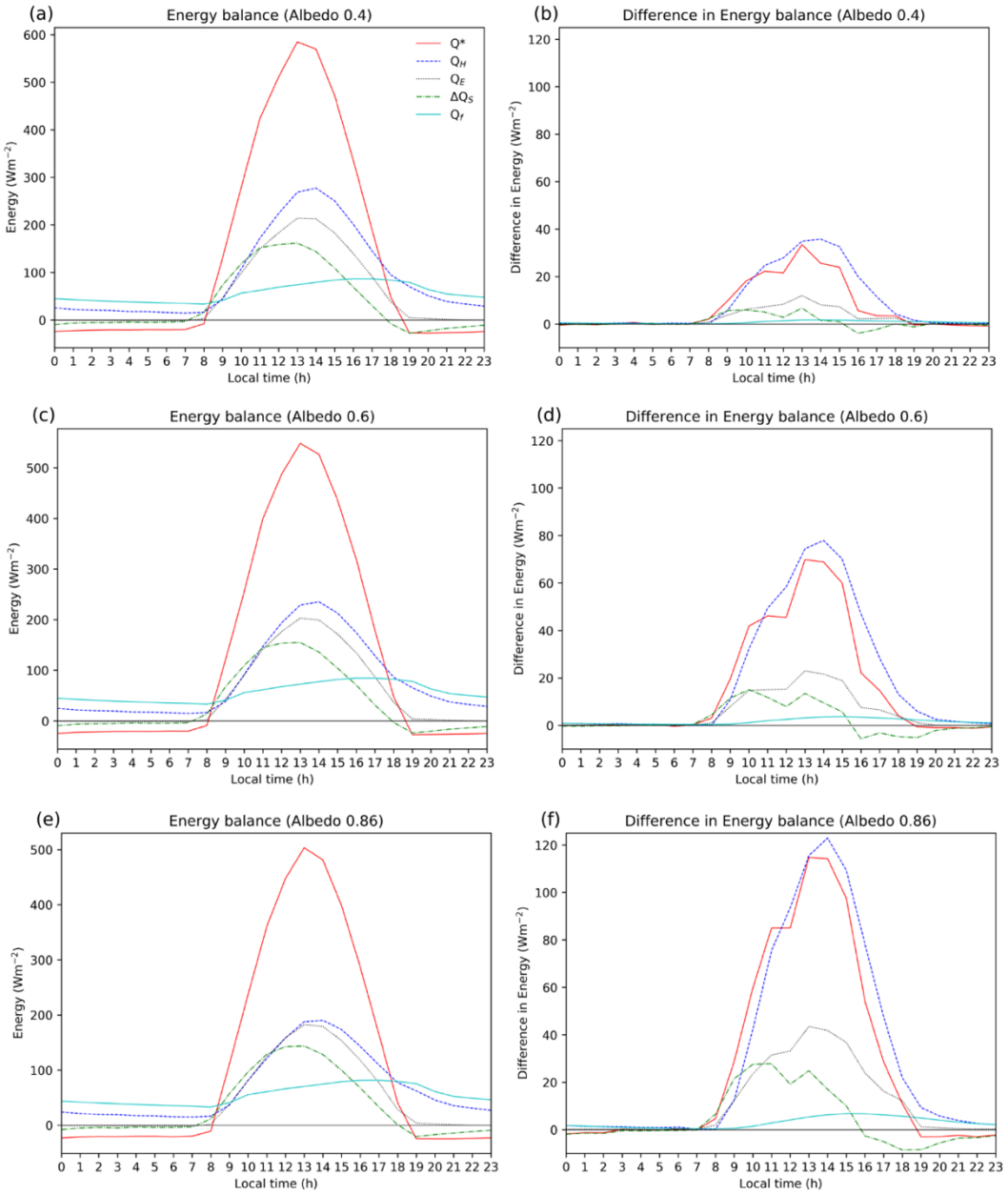

Fig 4 Surface energy balance averaged over the entire built-up area of Singapore for cases with roof albedo values of (a) 0.4, (c) 0.6 and (e) 0.86 and difference in energy balance between the Control case and cases with roof albedo values of (b) 0.4, (d) 0.6 and (f) 0.86.

The comparison of the Control case (albedo 0.2) (Fig. 5a) and the Cool roof case with albedo 0.86 (Fig. 5b) shows that adopting cool roofs can mitigate the effect of the thermal

Formatted: Fo
Deleted: 5
Deleted: 5
Formatted: Fo

stress in the tropical environment. The city-wide deployment of cool roofs reduced the *HI* by about 2-2.5 °C (Fig. 5c) at 14:00 LT in LCZ 9 and LCZ 10 mostly in the Northern and Western sectors of Singapore. Heat stress in those sectors changed from the range of "extreme caution" to "caution", reducing the adverse impact on the health of Singaporean inhabitants and improving the overall thermal comfort.

Formatted: Fo

Deleted: 5

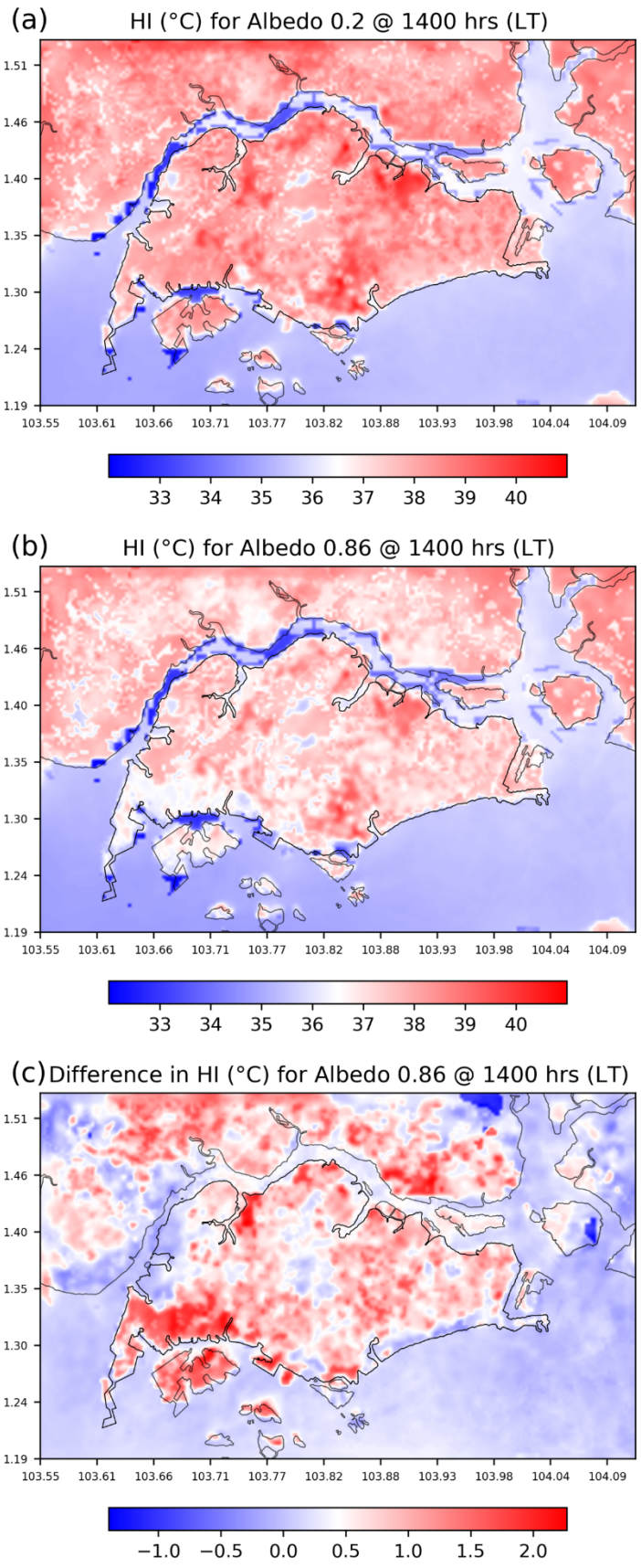
(a)
HI (°C) for Albedo 0.2 @ 1400 hrs (LT)
1.51
1.46
1.40
1.35
1.30
1.24
1.19
103.55 103.61 103.66 103.71 103.77 103.82 103.88 103.93 103.98 104.04 104.09
33 34 35 36 37 38 39 40
(b)
HI (°C) for Albedo 0.86 @ 1400 hrs (LT)
1.51
1.46
1.40
1.35
1.30
1.24
1.19
103.55 103.61 103.66 103.71 103.77 103.82 103.88 103.93 103.98 104.04 104.09
33 34 35 36 37 38 39 40
(c)
Difference in HI (°C) for Albedo 0.86 @ 1400 hrs (LT)
1.51
1.46
1.40
1.35
1.30
1.24
1.19
103.55 103.61 103.66 103.71 103.77 103.82 103.88 103.93 103.98 104.04 104.09
−1.0 −0.5 0.0 0.5 1.0 1.5 2.0

Fig. 5 Spatial distribution of averaged *HI* for (a) the Control (albedo value 0.2); (b) albedo 0.86; and (c) difference of the Control case and cool roof case with albedo 0.86.

3.2.2 Effect of modifying indoor thermostat set temperature

The city-wide comparison of the simulated sensible heat fluxes for the Control and the ITIT case for each LCZ is shown in Fig. 6a,b, respectively. The AC system in the ITIT case reduced the sensible heat fluxes exchanged with the atmosphere compared with the Control case. The waste heat rejected by the AC systems in the Control case contributed to a peak total sensible heat flux above 224 Wm^{-2} for LCZ 1 (16:00 LT); in this LCZ type the increased thermostat set point reduced the sensible heat flux by 46.6 Wm^{-2}, which translates into 20.6 % reduction in energy consumption during the evening. The AC consumption island-wide reduces by ~1689 MW (Fig S8). The largest savings of 989 MW are obtained in LCZ 4 at 16:00 LT, LCZs 5 and 8 also show sufficient savings (275 and 132 MW, respectively) in the ITIT case but savings in other LCZ are comparatively lower.

The reduction in the waste heat released from the ACs also impacted the UHI intensities for the Control and ITIT case as shown in Fig. 6c,d, respectively. The UHI intensities were particularly reduced for LCZ 1 from 3.6 °C at 00:00 LT to about 3.4 °C.

Formatted: Fo
Deleted: 6
Deleted: 6
Formatted: Fo

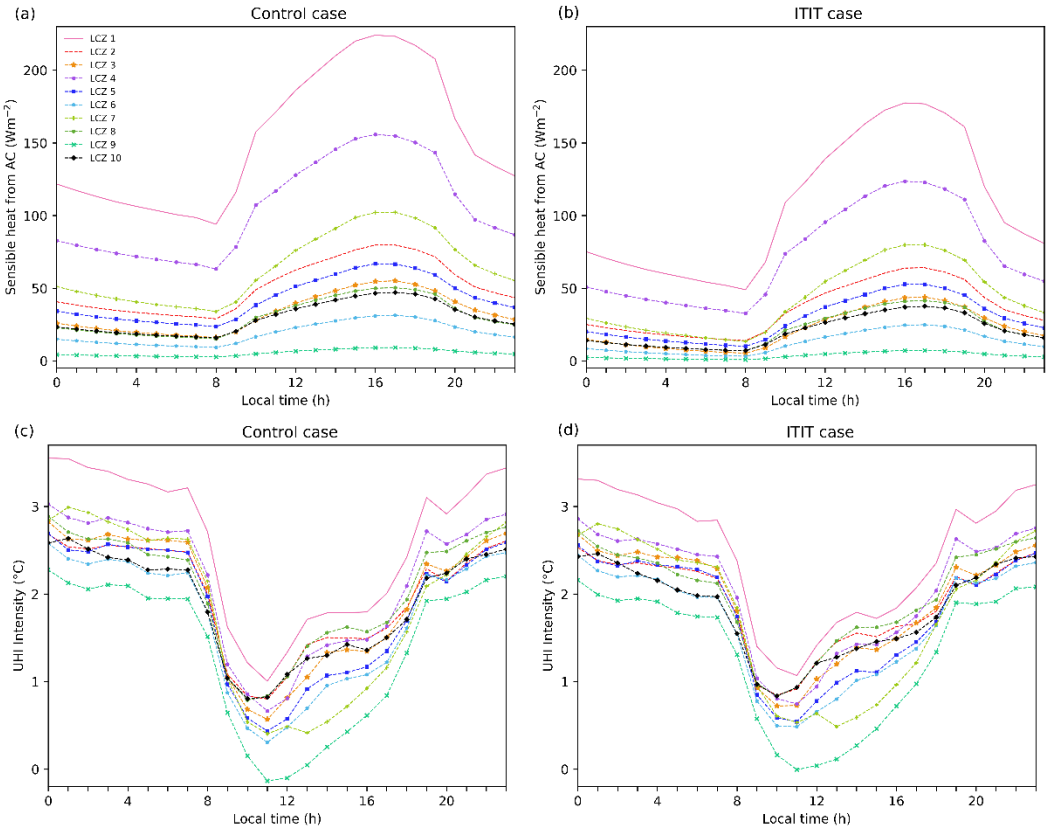

Fig. 6 Comparison of (a), (b): the sensible heat flux from the AC systems and (c), (d): UHI intensity of each LCZ class for Control and ITIT cases

The Control case and ITIT simulations were also compared with the NoAH experiment in order to evaluate the contribution of the AC systems to air temperature. Fig. 7a-d shows the mean spatial 2-m air temperature difference (Control - NoAH and ITIT - NoAH) averaged over the entire month of April 2016. During night and early morning (from 20:00 to 05:00 LT) (Fig. 7a,b), the effect of the AC systems was significant, increasing the mean 2-m air temperature by 1 °C in most parts of the city and up to 3 °C for the city center and for some parts in the Northeast and Southwest. It is also worth noting that the temperature increase was higher for the Control case compared to that for the ITIT case, which again indicated the importance of increasing the thermostat set temperature in buildings

Formatted: Fo
Deleted: 7
Deleted: 7
Formatted: Fo

particularly in the commercial areas. During daylight hours (07:00 to 19:00 LT) the effect of AC systems was less, with near-surface temperature differences below 1.5 °C for most parts of the city (Fig. 7c,d).

Formatted: Fo

Deleted: 7

The diurnal profile of ensemble mean PBL height averaged by LCZ type is influenced by the AH from the AC systems (see Fig. S7a-S7c). In the absence of AH, all LCZs show almost equal PBL height during early morning. Lower PBL heights are observed in all LCZs in the ITIT case due to lower AH during early morning. The PBL height decays more quickly for all LCZs in the Control case during nighttime compared to the ITIT case. It should be noted that the peak PBL height for LCZ 1 is much higher compared to the peak PBL height of LCZ 8 due to higher building surface fraction and the associated AH flux.

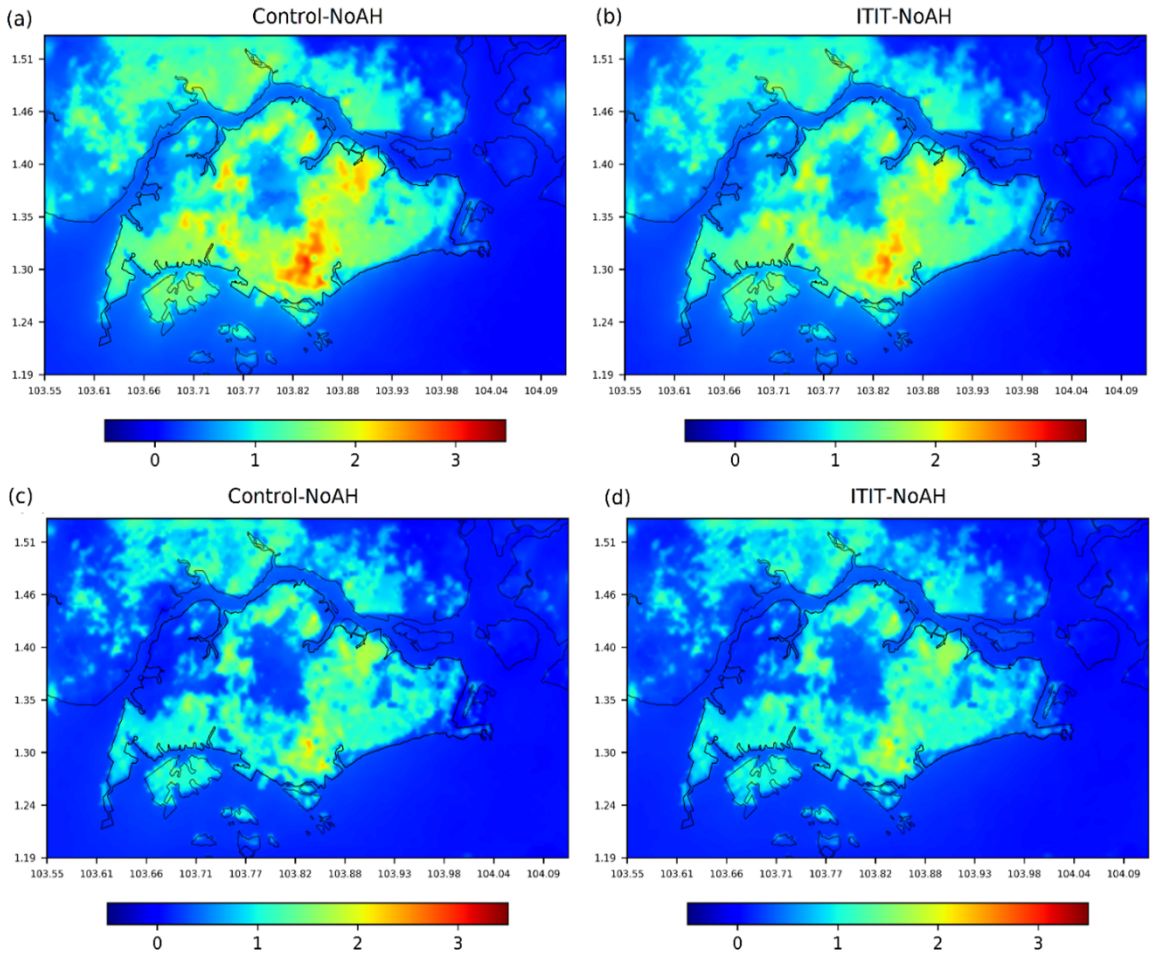

Fig. 7 Mean 2-m air temperature differences between the (a) Control, (b) ITIT and NoAH cases averaged over April 2016 during nighttime hours. (c) and (d) are the same as (a) and (b) except for daytime hours.

As stated earlier that the energy consumption from the WRF model is only indicative. To understand WRF's performance in simulation the energy consumption, the simulated energy consumption is compared against the Singapore's electricity system demand data (Fig .Fig. 8). It should be noted that simulated energy consumption only includes the electricity demand from the buildings (AC system), while Singapore's electricity system demand considers the whole island including the industry. The model underestimates the energy consumption during night time but overestimates it during the day time due to (1) the various assumptions made (e.g. choice of the indoor set temperature, time of the AC operation) can substantially overestimate the electricity demand; (2) excluding industrial energy consumption can seriously underestimate the electricity demand. It can be seen clearly that ITIT case requires much less energy consumption than the control case and therefore can be considered as an effective mitigation measure.

Deleted: 8

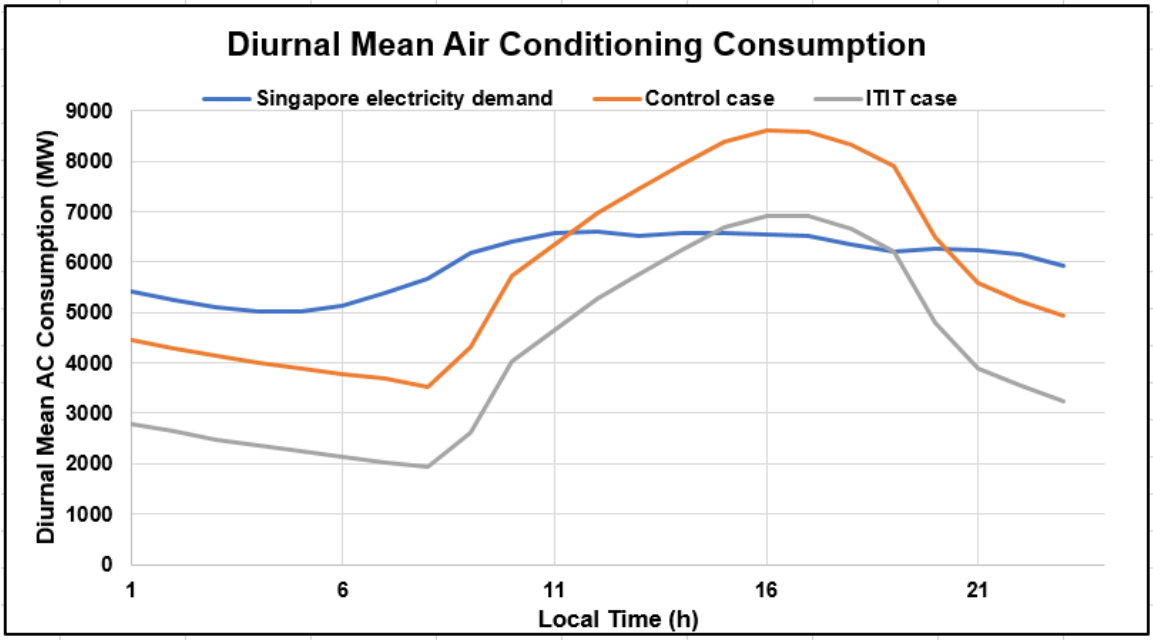

Fig. 8 Comparison of the Singapore's averaged diurnal electricity system demand for April 2016 against WRF-simulated AC demand from the Control and ITIT cases.

3.2.3 Urban densification

By 2030, Singapore's total population could range between 6.5 and 6.9 million (*National Population and Talent Division*, 2013). In order to accommodate the increase in population density from approximately 7,841 people/km^2 (2016) to 9,040-9,600 people/km^2 (2030), the Urban Redevelopment Authority (URA) of Singapore is considering densifying some existing areas currently classified as "Open" LCZs, which will shift them to "Compact" classes. Based on URA's 2014 master plan (URA, 2016), a new LCZ map (Fig. 9 a) was developed. Compared to the previous LCZ classification, the level of densification varies in each LCZ class as demonstrated by the comparison between the Control and densification scenarios in Fig. 9 b. It is evident that percentage coverage for LCZ 1, 6, and 10 increased in the densification scenario, while that for LCZ 2, 5 and 8 decreased. The URA-based classification has also reduced the number of LCZ classes in the built-up area of Singapore (compared to the initial LCZ classification) and LCZs 3, 4 and 9 have been replaced by LCZ 1. LCZ 8 has been primarily replaced by LCZ 10 while LCZ 7 has been taken over by LCZ 8. The reclaimed land which will be developed as a mega-port in Southwest Singapore (Tuas) by 2021 is also included as LCZ 8. The Tanjong Pagar terminal located in the South of the city has been changed from LCZ 7 to LCZ 8.

The diurnal variation of the difference in air temperature between the Control case and the densification case for each LCZ is shown in Fig. 10 . The simulated results show that this densification would lead to rise in temperature of about 1.4 ºC (averaged spatially over the urban classes for month of April 2016) compared to the Control case for LCZ 1. One

Deleted: 9
Formatted: Fo
Deleted: 9
Formatted: Fo
Formatted: Fo
Deleted: 10

reason for this temperature rise is the blockage of main ventilation corridors (NUS 2012; Ng and Ren, 2015) (as most of the open dwellings are replaced by compact high-rise areas) and the increased heat storage due to increased building volume. Another important factor of this temperature rise is the increase in the waste heat released per floor from AC systems due to increased heat per ground area. The radiation trapping, however, is reduced as the shading is increased in the urban canyon due to tall towers (Li *et al.*, 2020). Densification also impacts the diurnal profile of the PBL height (Fig. S7d). The peak PBL heights increase for all LCZs compared to the Control case. During early morning the PBL heights in the densification scenarios are also higher compared to the Control case except for LCZ 5. The PBL height of LCZ 5 also decays quickly in the night which might be due to its reduced percentage coverage in the densification scenario.

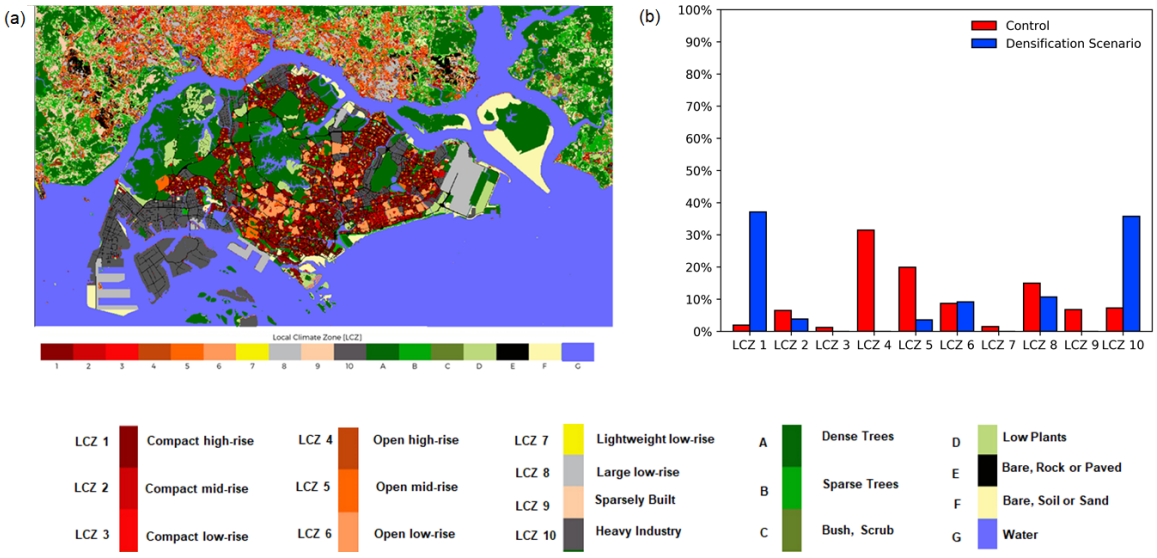

Fig. 9 (a) LCZ map 2030 and (b) percentage coverage of different LCZ classes between the Control and densification scenarios

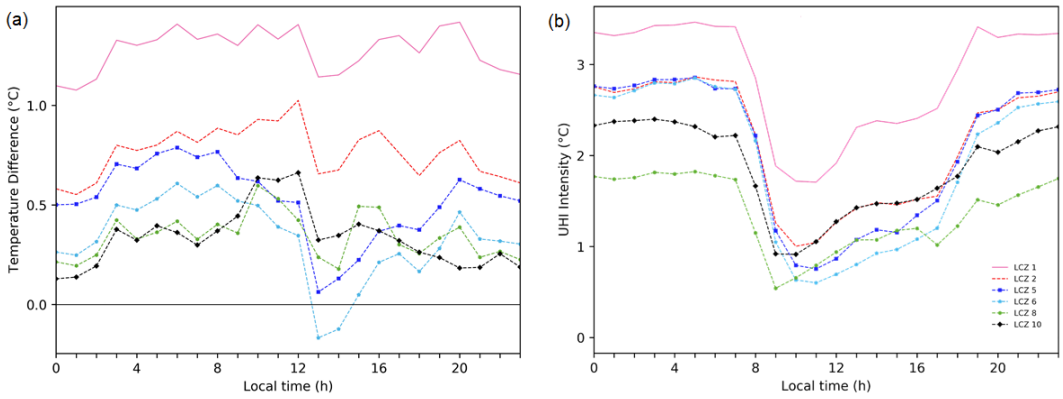

Fig. 10 (a) Diurnal variation of the temperature difference between the densification and Control cases; (b) Diurnal variation of the UHI intensity (densification - AllGreenMod).

The UHI intensity for the densification scenario is shown in Fig. 10. By increasing the extent of LCZ 1 (comparing Fig. 6c and Fig. 10 b), the UHI intensity had increased particularly from 03:00 to 14:00 LT, to a magnitude of 0.68°C compared to that of the Control case. The obvious reason for this increase was the increased building volume, blockage of the main wind corridors and the reduced wind speed due to increased drag. Compared with the UHI intensity for the Control case, the UHI for the densification case decreased from 20:00 LT, then started increasing from 03:00 LT and stayed mostly higher for the rest of day until 19:00 LT. The reduced UHI intensity during the night was due to the increased extent of LCZ 10 areas, which allowed more rapid heat dissipation with low-rise industrial buildings and almost no vegetation compared to the Control case; however, the persistent increase during the daytime was due to increased paved area.

Deleted: 10
Formatted: Fo
Deleted: 6
Formatted: Fo
Formatted: Fo
Deleted: 10

The UHI intensities for LCZs 2, 5 and 6 were higher during 00:00 LT to 07:00 LT. The peak UHI intensity difference for all these LCZs was at 05:00 LT (LCZ 6 had the highest, 0.66°C). LCZ 2 had less extent in the densification case compared to the Control case, but due to the reduced shading in the densification case, more heat was trapped in this

LCZ. The trapped heat in urban areas tends to be released slower in the night, and therefore LCZ 2 had higher UHI intensity. The reduction in LCZ 5 in the densification scenario compared to the control case led to an increase in UHI. This could be due to decreased shading from the buildings and vegetation cover. A small increase in LCZ 6 in the densification scenario increased UHI due to the increasing building coverage compared to vegetation and more cooling loads. LCZ 8 had lower UHI than that in the Control case during late night due to more radiation trapping in the Control case. The nighttime as well as the midday temperatures were higher for LCZ 8, which, as explained earlier, was due to more radiation trapping.

4. Discussion

4.1 *UHI pattern*

The detailed analysis of UHI was presented in our earlier study (Mughal et al., 2019). The UHI intensities are higher compared to that reported by Li et al. (2013), possibly because April 2016 is a very hot period, with a record-setting maximum temperature 36.4 °C (Meteorological Service Singapore, 2017). Higher temperatures in LCZ 1 (Compact High Rise) and lower temperatures in LCZ 9 (Sparsely Built) are consistent with the findings of Ng (2015). Both Ng (2015) and the present study reported negative UHI intensity in Sparsely Built (LCZ 9) areas in Singapore, with their difference of magnitude caused by the time of year and the spatial/temporal averaging over urban pixels in the present study. The spatial distribution of the UHI intensity is also consistent with the finding from Li et al. (2013). A survey of the nocturnal UHI was conducted by Wong and Yu (2005) in Singapore based on an island-wide traverse in September between 02:00 and 04:00 LT. They also found a UHI intensity of ~4°C, measured as the difference between

the CBD and the forested central catchment. The overall UHI intensity from our study is within the range for the tropics (~4 °C), as summarized in Roth (2007).

4.2 Cool roof

According to Li and Norford, (2016), cool roofs reduce the near surface air temperature by a maximum of 1.8 °C in the industrial/commercial area; in the present study a maximum of 1.3 °C in LCZ 8 (Large Low Rise) is achieved. The different temperature reduction between these two studies is caused by the different LULC and the exclusion of AH in Li and Norford (2016). Both studies showed that the energy balance components have comparable maximum and minimum values and are peaking and dipping at the same time. The net radiation, sensible and latent heat fluxes are following the same pattern during day and night as reported in Sharma et al. (2016). The city-wide application of cool roof reduced the daytime near surface UHI intensity significantly (up to 1.3°C) as reported in Li et al. (2014). There, however, may be some other impacts caused by cool roof deployment. For example, with the cooling at the surface, the vertical mixing will be reduced, and the atmospheric stability will be enhanced. The PBL height will therefore be reduced, and this will affect pollutant dispersion in urban areas (Li et al., 2016). As pointed out by Yang and Bou-Zeid (2019), the effectiveness of the cool roofs depend on the deployment scale, time of the day, wind pattern and the albedo value utilized. It is observed in our study that the city-wide deployment of the cool roofs provided effective reduction in the 2m air temperature (heat mitigation) in Singapore. When only a part of the city is implemented, the cooling effect should be lower. Therefore, the results reported here should be taken as an upper limit of cool roofs with the specific albedo values.

4.3. Indoor thermostat set-point temperature

The contribution of AH to UHI for the Control case is discussed in detail in Mughal et al. (2019). Previous work (e.g., De Munck et al., 2013; Salamanca et al., 2012,2014) has reported that the AC systems impacted the regional climatology more during night due to the limited depth of the urban boundary layer. A smaller quantity of heat rejected during night can induce higher increase in the air temperature than that by a greater quantity released during the day (Salamanca et al., 2014). Consistently, we also find more significant impact of AC systems on nighttime temperatures than daytime temperature. It is found in the present study that the increase in the indoor set temperature to 25 °C can reduce UHI by about 0.2 - 0.4 °C and the waste heat by about 20 - 25 Wm^{-2}. The energy consumption can be reduced by about 20%, similar to that reported in Pokhrel et al. (2019). The results in the present study revealed that the lower thermostat set-point temperature for AC systems could exacerbate the nocturnal UHI and deteriorate outdoor thermal comfort.

4.4. Urban densification

Warming induced by urban expansion depends on the trajectory of development (Georgescu *et al.*, 2013). Li et al. (2016) found that the asymmetric patterns of urbanization in Singapore can increase the UHI intensity. Adachi et al. (2014) detected 0.5 °C increase in air temperature when Tokyo expanded compared with a compact scenario. In the present study, we only considered the temperature rise due to the compactness introduced in Singapore, which is about 1.4 °C. Nichol et al. (2014) estimated that daytime temperatures in highly urbanized areas in Hong Kong will rise by 2 °C in 2039, which is somewhat comparable to our results. Georgescu et al. (2013) showed that megapolitan expansion in the U.S., alone and separate from greenhouse gas-induced forcing, can be expected to raise near-surface temperatures by 1–2 °C. Fortunately, Georgescu et al. (2014) also

demonstrated that by taking adaptive measures (green, cool roof, and hybrid approaches), it is possible to roll back the warming effects caused by city expansion. To accommodate economic development and projected population increase by 2030, the inevitable urban densification in Singapore should be accompanied with appropriate UHI mitigation measures. In future work we intend to characterize scenarios considering both urban expansion and global climate change (e.g., Adachi et al., 2014; Nichol et al., 2014), as well as the mitigation effects of various measures in these scenarios.

5. Conclusions

Previous studies have shown that Singapore's canopy layer UHI intensity can reach up to 5 ºC in compact areas during night. Using the validated WRF/MLUCM model, this study evaluated several mitigation scenarios that would help counteract the UHI effect in Singapore. The local climate zone (LCZ) map of Singapore was used as land use data to explore the intra-urban variability of the impact of mitigation measures.

One of the prominent mitigation measures in this study was increasing the albedo value of roofs (0.2) incrementally to a maximum possible value (0.86). The associated UHI, surface energy balance and heat indices were examined in detail and uncomfortable thermal locations were identified. A maximum cooling effect of 1.3 °C at 13:00 LT (Fig. 2h) and a maximum reduction of 1.3 °C in UHI intensity were observed in LCZ 8 when cool roofs of albedo 0.86 were deployed. By considerably lowering heat storage, cool roofs could lower cooling loads and reduce anthropogenic heat releases. The city-wide deployment of cool roofs reduced the heat index by about 2-2.5 °C at noon in LCZ 9 and 10 (mostly in the Northern and Western areas of Singapore), hence changing them from the range of "extreme caution" to "caution" and reducing human heat stress.

Formatted: Fo

Deleted: 2

The AC systems' contribution to the waste heat released to the urban environment had significant effect on 2-m air temperature during the night. When there was no anthropogenic heat due to AC systems, the mean 2-m air temperature showed a reduction of more than 1 °C in most parts of the city. This effect could be mitigated by increasing the thermostat set temperature from 21 to 25 °C. The UHI intensities were particularly reduced for LCZ 1 from 3.6 °C at 00:00 LT to about 3.4 °C and the 2-m air temperature was reduced by about 0.36 °C at 08:00 LT. The maximum reduction of 46.6 Wm^{-2} in the anthropogenic sensible heat flux was observed during evening for LCZ 1, which translated into 20.6% reduction in the energy consumption during evening.

A future (2030) densification scenario was also analyzed in this study without considering future climate change, to demonstrate how UHI can be deteriorated if Singapore is densified. With a new LCZ classification based on the 2014 master plan and the same synoptic conditions, an increase of 1.4 °C in LCZ 1 was observed when compared with the simulation using the current LCZ map. The UHI intensity also increased in LCZ 1 due to the increased building volume, blockage of the main wind corridors and the reduced wind speed due to increased drag. The scenario demonstrated the necessity to limit the densification of less compact areas for a thermally comfortable future in Singapore even without considering future climate change, and the importance of deploying UHI mitigation measures if urban densification is inevitable.

The results from this study could help planners and developers improve building construction designs in thermally comfort zones and avoid development in hot spots. This study also provides some guidance on possible future densification scenarios by estimating the impact on thermal comfort and UHI of such densifications. In addition to those

evaluated in this study, there are still many available mitigation measures, including greenery and trees (either on the street or roofs) (Liu et al., 2017), yet to be investigated. Considering the general method and model used in this study, these results could also be applied to cities with similar climates and help in evaluating the available UHI mitigation measures. Our future work will evaluate these mitigation effects by considering future climate changes under different greenhouse gas emission scenarios.

Acknowledgments. This research is supported by the National Research Foundation Singapore (NRF) under its Campus for Research Excellence and Technological Enterprise (CREATE) programme and its Intra-CREATE Collaborative Grant "Cooling Singapore." The Center for Environmental Sensing and Modeling (CENSAM) is an interdisciplinary research group of the Singapore-MIT Alliance for Research and Technology (SMART). We acknowledge Mr. Elliot Koh Jing Yao for his help in plotting some of the figures.

REFERENCES

Adachi, S. A., Kimura, F., Kusaka, H., Duda, M. G., Yamagata, Y., Seya, H., Nakamichi, K. and Aoyagi, T. (2014) 'Moderation of summertime heat island phenomena via modification of the urban form in the Tokyo metropolitan area', *Journal of Applied Meteorology and Climatology*, 53(8), pp. 1886–1900.

Aflaki, A., Mirnezhad, M., Ghaffarianhoseini, Amirhosein, Ghaffarianhoseini, Ali, Omrany, H., Wang, Z.-H. and Akbari, H. (2017) 'Urban heat island mitigation strategies: A state-of-the-art review on Kuala Lumpur, Singapore and Hong Kong', *Cities*. Elsevier, 62, pp. 131–145.

Bechtel, B., Alexander, P. J., Böhner, J., Ching, J., Conrad, O., Feddema, J., Mills, G., See, L. and Stewart, I. (2015) 'Mapping local climate zones for a worldwide database of the form and function of cities', *ISPRS International Journal of Geo-Information*. Multidisciplinary Digital Publishing Institute, 4(1), pp. 199–219.

Bohnenstengel, S. I., Evans, S., Clark, P. A. and Belcher, S. E. (2011) 'Simulations of the London urban heat island', *Quarterly Journal of the Royal Meteorological Society*. Wiley Online Library, 137(659), pp. 1625–1640.

Bougeault, P. and Lacarrere, P. (1989) 'Parameterization of orography-induced turbulence in a mesobeta--scale model', *Monthly Weather Review*, 117(8), pp. 1872–1890.

Buzan, J. R., Oleson, K. and Huber, M. (2015) 'Implementation and comparison of a suite of heat stress metrics within the Community Land Model version 4.5', *Geoscientific Model Development*. Copernicus GmbH, 8(2), pp. 151–170.

Chen, F. and Dudhia, J. (2001) 'Coupling an advanced land surface–hydrology model with the Penn State–NCAR MM5 modeling system. Part I: Model implementation and sensitivity', *Monthly Weather Review*, 129(4), pp. 569–585.

Chen, F., Yang, X. and Zhu, W. (2014) 'WRF simulations of urban heat island under hot-weather synoptic conditions: The case study of Hangzhou City, China', *Atmospheric research*. Elsevier, 138, pp. 364–377.

Chen, L., Zhang, M. and Wang, Y. (2016) 'Model analysis of urbanization impacts on boundary layer meteorology under hot weather conditions: a case study of Nanjing, China', *Theoretical and applied climatology*. Springer, 125(3–4), pp. 713–728.

Chew, L. W., Liu, X., Li, X.-X. and Norford, L. K. (2021) 'Interaction between heat wave and urban heat island: A case study in a tropical coastal city, Singapore', *Atmospheric Research*, 247, p. 105134. doi: https://doi.org/10.1016/j.atmosres.2020.105134.

Ching, J., See, L., Mills, G., Alexander, P., Bechtel, B., Feddema, J., Oleson, K. L., Stewart, I., Neophytou, M. and Chen, F. (2014) 'WUDAPT: Facilitating advanced urban canopy modeling for weather, climate and air quality applications', in *94th American Meterological Society Annual Meeting*. Georgia, USA.

Ching, J., Mills, G., Bechtel, B., See, L., Feddema, J., Wang, X., Ren, C., Brousse, O., Martilli, A. and Neophytou, M. (2018) 'World urban database and access portal tools (WUDAPT), an urban weather, climate and environmental modeling infrastructure for the anthropocene', *Bulletin of the American Meteorological Society*, (2018).

Chow, W. T. L. and Roth, M. (2006) 'Temporal dynamics of the urban heat island of Singapore', *International Journal of climatology*. Wiley Online Library, 26(15), pp. 2243–2260.

Chua, K. J., Chou, S. K., Yang, W. M. and Yan, J. (2013) 'Achieving better energy-

efficient air conditioning–a review of technologies and strategies', *Applied Energy*. Elsevier, 104, pp. 87–104.

Damiati, S. A., Zaki, S. A., Wonorahardjo, S., Wong, N. H. and Rijal, H. B. (2015) 'Comfort Temperature in Air Conditioned Office Buildings: Case Study of Indonesia And Singapore', in *Malaysia-Japan Joint International Conference 2015 (MJJIC2015)*.

Dudhia, J. (1989) 'Numerical study of convection observed during the winter monsoon experiment using a mesoscale two-dimensional model', *Journal of the atmospheric sciences*, 46(20), pp. 3077–3107.

Fallmann, J. (2014) 'Numerical simulations to assess the effect of urban heat island mitigation strategies on regional air quality'. Universität zu Köln.

Fallmann, J., Suppan, P. and Emeis, S. (2013) 'Modeling of the Urban Heat Island (UHI) using WRF-Assessment of adaptation and mitigation strategies for the city of Stuttgart.', in *EGU General Assembly Conference Abstracts*.

Fischer, E. M. and Schär, C. (2010) 'Consistent geographical patterns of changes in high-impact European heatwaves', *Nature Geoscience*. Nature Publishing Group, 3(6), p. 398.

Fong, M. and Ng, L. K. (2012) *The weather and climate of Singapore*. Meteorological Service Singapore.

Georgescu, M., Moustaoui, M., Mahalov, A. and Dudhia, J. (2013) 'Summer-time climate impacts of projected megapolitan expansion in Arizona', *Nature Climate Change*. Nature Publishing Group, 3(1), p. 37.

Georgescu, M., Morefield, P. E., Bierwagen, B. G. and Weaver, C. P. (2014) 'Urban

adaptation can roll back warming of emerging megapolitan regions', *Proceedings of the National Academy of Sciences*. National Acad Sciences, 111(8), pp. 2909–2914.

González-Aparicio, I., Baklanov, A., Hidalgo, J., Korsholm, U., Nuterman, R. and Mahura, A. (2014) 'Impact of city expansion and increased heat fluxes scenarios on the urban boundary layer of Bilbao using Enviro-HIRLAM', *Urban Climate*. Elsevier, 10, pp. 831–845.

Kain, J. S. (2004) 'The Kain–Fritsch convective parameterization: an update', *Journal of Applied Meteorology*, 43(1), pp. 170–181.

Keung, J. (2010) *Building and Construction Authority. Building Planning and Massing. Green Building Platinum Series*. Available at: https://www.bca.gov.sg/GreenMark/others/bldgplanningmassing.pdf.

Kikegawa, Y., Genchi, Y., Yoshikado, H. and Kondo, H. (2003) 'Development of a numerical simulation system toward comprehensive assessments of urban warming countermeasures including their impacts upon the urban buildings' energy-demands', *Applied Energy*. Elsevier, 76(4), pp. 449–466.

Kim, W. W. (2018) *Population trends 2018*. Singapore. Available at: https://www.singstat.gov.sg/-/media/files/publications/population/population2018.pdf.

Kusaka, H., Kondo, H., Kikegawa, Y. and Kimura, F. (2001) 'A simple single-layer urban canopy model for atmospheric models: Comparison with multi-layer and slab models', *Boundary-layer meteorology*. Springer, 101(3), pp. 329–358.

Leal Filho, W., Echevarria Icaza, L., Emanche, V. O. and Quasem Al-Amin, A. (2017) 'An

evidence-based review of impacts, strategies and tools to mitigate urban heat islands', *International journal of environmental research and public health*. Multidisciplinary Digital Publishing Institute, 14(12), p. 1600.

Li, D. and Bou-Zeid, E. (2014) 'Quality and sensitivity of high-resolution numerical simulation of urban heat islands', *Environmental Research Letters*. IOP Publishing, 9(5), p. 55001.

Li, D., Bou-Zeid, E. R. and Oppenheimer, Michael (2014) 'The effectiveness of cool and green roofs as urban heat island mitigation strategies', *Environmental Research Letters*. IOP Publishing Ltd., 9(5), p. 55002.

Li, X.-X. (2018) 'Linking residential electricity consumption and outdoor climate in a tropical city', *Energy*. Elsevier.

Li, X.-X., Britter, R. and Norford, L. K. (2016) 'Effect of stable stratification on dispersion within urban street canyons: A large-eddy simulation', *Atmospheric Environment*. Elsevier, 144, pp. 47–59.

Li, X.-X. and Norford, L. K. (2016) 'Evaluation of cool roof and vegetations in mitigating urban heat island in a tropical city, Singapore', *Urban Climate*. Elsevier, 16, pp. 59–74.

Li, X., Koh, T., Entekhabi, D., Roth, M., Panda, J. and Norford, L. K. (2013) 'A multi-resolution ensemble study of a tropical urban environment and its interactions with the background regional atmosphere', *Journal of Geophysical Research: Atmospheres*. Wiley Online Library, 118(17), pp. 9804–9818.

Li, X., Koh, T., Panda, J. and Norford, L. K. (2016) 'Impact of urbanization patterns on the local climate of a tropical city, Singapore: An ensemble study', *Journal of*

Geophysical Research: Atmospheres. Wiley Online Library, 121(9), pp. 4386–4403.

Li, Y., Schubert, S., Kropp, J. P. and Rybski, D. (2020) 'On the influence of density and morphology on the Urban Heat Island intensity', *Nature communications*. Nature Publishing Group, 11(1), pp. 1–9.

Liu, X., Li, X.-X., Harshan, S., Roth, M. and Velasco, E. (2017) 'Evaluation of an urban canopy model in a tropical city: the role of tree evapotranspiration', *Environmental Research Letters*. IOP Publishing, 12(9), p. 94008.

Martilli, A. (2002) 'Numerical study of urban impact on boundary layer structure: Sensitivity to wind speed, urban morphology, and rural soil moisture', *Journal of Applied Meteorology*, 41(12), pp. 1247–1266.

Martilli, A., Brousse, O. and Ching, J. (2016) *Urbanized WRF modeling using WUDAPT*. Technical Report March, Cientro de Investigaciones Energeticas MedioAmbientales y Tecnologicas (CIEMAT), Madrid.

Masson, V. (2006) 'Urban surface modeling and the meso-scale impact of cities', *Theoretical and applied climatology*. Springer, 84(1–3), pp. 35–45.

Meteorological Service Singapore (2017) *Annual climatological report 2016*. Signapore. Available at: http://www.weather.gov.sg/wp-content/uploads/2017/02/Annual-Climatological-Report-2016.pdf.

Miao, S., Chen, F., LeMone, M. A., Tewari, M., Li, Q. and Wang, Y. (2009) 'An observational and modeling study of characteristics of urban heat island and boundary layer structures in Beijing', *Journal of Applied Meteorology and Climatology*, 48(3), pp. 484–501.

Miller, R. B. and Small, C. (2003) 'Cities from space: potential applications of remote sensing in urban environmental research and policy', *Environmental Science & Policy*. Elsevier, 6(2), pp. 129–137.

Mills, G., Ching, J., See, L., Bechtel, B. and Foley, M. (2015) 'An Introduction to the WUDAPT project', in *Proceedings of the 9th International Conference on Urban Climate, Toulouse, France*, pp. 20–24.

Mirzaei, P. A. (2015) 'Recent challenges in modeling of urban heat island', *Sustainable cities and society*. Elsevier, 19, pp. 200–206.

Mlawer, E. J., Taubman, S. J., Brown, P. D., Iacono, M. J. and Clough, S. A. (1997) 'Radiative transfer for inhomogeneous atmospheres: RRTM, a validated correlated-k model for the longwave', *Journal of Geophysical Research: Atmospheres*. Wiley Online Library, 102(D14), pp. 16663–16682.

Monin, A. S. and Obukhov, A. M. (1954) 'Basic laws of turbulent mixing in the surface layer of the atmosphere', *Contrib. Geophys. Inst. Acad. Sci. USSR*, 151(163), p. e187.

Mughal, M. O., Li, X.-X., Yin, T., Martilli, A., Brousse, O., Dissegna, M. . and Norford, L. . (2019) 'High-resolution, multi-layer modelling of Singapore's urban climate incorporating local climate zones', *Journal of Geophysical Research: Atmospheres*, 124. doi: 10.1029/2018JD029796.

De Munck, C., Pigeon, G., Masson, V., Meunier, F., Bousquet, P., Tréméac, B., Merchat, M., Poeuf, P. and Marchadier, C. (2013) 'How much can air conditioning increase air temperatures for a city like Paris, France?', *International Journal of Climatology*. Wiley Online Library, 33(1), pp. 210–227.

National Centers for Environmental Prediction, National Weather Service, NOAA, U. . D. of C. (2015) 'NCEP GDAS/FNL 0.25 Degree Global Tropospheric Analyses and Forecast Grids'. Boulder, CO: Research Data Archive at the National Center for Atmospheric Research, Computational and Information Systems Laboratory. doi: 10.5065/D65Q4T4Z.

National Population and Talent Division (2013) *A sustainable population for a dynamic Singapore: Population white paper*. Singapore. Available at: http://population.sg/whitepaper/resource-files/population-white-paper.pdf (Accessed: 20 August 2018).

Ng, E. and Ren, C. (2015) *The urban climatic map: A methodology for sustainable urban planning*. Routledge.

Ng, Y. X. Y. (2015) 'A Study of Urban Heat Island using "Local Climate Zones"–The Case of Singapore.'

Nichol, J., Hang, T. P. and Ng, E. (2014) 'Temperature projection in a tropical city using remote sensing and dynamic modeling', *Climate dynamics*. Springer, 42(11–12), pp. 2921–2929.

NUS (2012) *Urban climatic mapping study*. Singapore.

Ohashi, Y., Genchi, Y., Kondo, H., Kikegawa, Y., Yoshikado, H. and Hirano, Y. (2007) 'Influence of air-conditioning waste heat on air temperature in Tokyo during summer: numerical experiments using an urban canopy model coupled with a building energy model', *Journal of Applied Meteorology and climatology*, 46(1), pp. 66–81.

Phelan, P. E., Kaloush, K., Miner, M., Golden, J., Phelan, B., Silva III, H. and Taylor, R.

A. (2015) 'Urban heat island: mechanisms, implications, and possible remedies', *Annual Review of Environment and Resources*. Annual Reviews, 40, pp. 285–307.

Pisello, A. L. (2017) 'State of the art on the development of cool coatings for buildings and cities', *Solar Energy*. Elsevier, 144, pp. 660–680.

Pokhrel, R., Ramírez-Beltran, N. D. and González, J. E. (2019) 'On the assessment of alternatives for building cooling load reductions for a tropical coastal city', *Energy and Buildings*. Elsevier, 182, pp. 131–143.

Qiu, S., He, B., Zhu, Z., Liao, Z. and Quan, X. (2017) 'Improving Fmask cloud and cloud shadow detection in mountainous area for Landsats 4–8 images', *Remote Sensing of Environment*. Elsevier, 199, pp. 107–119.

Roth, M. (2007) 'Review of urban climate research in (sub) tropical regions', *Int J Climatol*. doi: 10.1002/joc.

Roth, M. and Chow, W. T. L. (2012) 'A historical review and assessment of urban heat island research in Singapore', *Singapore Journal of Tropical Geography*. Wiley Online Library, 33(3), pp. 381–397.

Rothfusz, L. P. (1990) 'The heat index equation (or, more than you ever wanted to know about heat index)', *Fort Worth, Texas: National Oceanic and Atmospheric Administration, National Weather Service, Office of Meteorology*, 9023.

Salamanca, F., Martilli, A., Tewari, M. and Chen, F. (2011) 'A study of the urban boundary layer using different urban parameterizations and high-resolution urban canopy parameters with WRF', *Journal of Applied Meteorology and Climatology*, 50(5), pp. 1107–1128.

Salamanca, F., Georgescu, M., Mahalov, A., Moustaoui, M. and Wang, M. (2014)

'Anthropogenic heating of the urban environment due to air conditioning', *Journal of Geophysical Research: Atmospheres*. Wiley Online Library, 119(10), pp. 5949–5965.

Salamanca, F. and Martilli, A. (2010) 'A new Building Energy Model coupled with an Urban Canopy Parameterization for urban climate simulations—part II. Validation with one dimension off-line simulations', *Theoretical and Applied Climatology*. Springer, 99(3–4), p. 345.

Salamanca, F., Martilli, A. and Yagüe, C. (2012) 'A numerical study of the Urban Heat Island over Madrid during the DESIREX (2008) campaign with WRF and an evaluation of simple mitigation strategies', *International Journal of Climatology*. Wiley Online Library, 32(15), pp. 2372–2386.

Sharma, A., Conry, P., Fernando, H. J. S., Hamlet, A. F., Hellmann, J. J. and Chen, F. (2016) 'Green and cool roofs to mitigate urban heat island effects in the Chicago metropolitan area: Evaluation with a regional climate model', *Environmental Research Letters*. IOP Publishing, 11(6), p. 64004.

Sharma, A., Fernando, H. J. S., Hamlet, A. F., Hellmann, J. J., Barlage, M. and Chen, F. (2017) 'Urban meteorological modeling using WRF: a sensitivity study', *International Journal of Climatology*. Wiley Online Library, 37(4), pp. 1885–1900.

Steadman, R. G. (1979) 'The assessment of sultriness. Part I: A temperature-humidity index based on human physiology and clothing science', *Journal of applied meteorology*, 18(7), pp. 861–873.

Tao, W., Wu, D., Lang, S., Chern, J., Peters-Lidard, C., Fridlind, A. and Matsui, T. (2016) 'High-resolution NU-WRF simulations of a deep convective-precipitation system

during MC3E: Further improvements and comparisons between Goddard microphysics schemes and observations', *Journal of Geophysical Research: Atmospheres*. Wiley Online Library, 121(3), pp. 1278–1305.

Tzavali, A., Paravantis, J. P., Mihalakakou, G., Fotiadi, A. and Stigka, E. (2015) 'Urban heat island intensity: a literature review', *Fresenius Environmental Bulletin*, 24, pp. 4535–4554.

URA (2016) *The planning act Master Plan written statement 2014*. Singapore. Available at: https://www.ura.gov.sg/-/media/User Defined/URA Online/master-plan/master-plan-2014/Written Statement 2014_uptd18jan16.pdf?la=en.

Wang, Y., Li, Y., Di Sabatino, S., Martilli, A. and Chan, P. W. (2018) 'Effects of anthropogenic heat due to air-conditioning systems on an extreme high temperature event in Hong Kong', *Environmental Research Letters*. IOP Publishing, 13(3), p. 34015.

Wen, Y. and Lian, Z. (2009) 'Influence of air conditioners utilization on urban thermal environment', *Applied Thermal Engineering*. Elsevier, 29(4), pp. 670–675.

Wong, N. H. and Yu, C. (2005) 'Study of green areas and urban heat island in a tropical city', *Habitat international*. Elsevier, 29(3), pp. 547–558.

World Health Organization (2018) *The world cities in 2018*. Available at: http://www.un.org/en/events/citiesday/assets/pdf/the_worlds_cities_in_2018_data_booklet.pdf.

Yang, J. and Bou-Zeid, E. (2019) 'Scale dependence of the benefits and efficiency of green and cool roofs', *Landscape and urban planning*. Elsevier, 185, pp. 127–140.

Zhao, L., Lee, X., Smith, R. B. and Oleson, K. (2014) 'Strong contributions of local

background climate to urban heat islands', *Nature*. Nature Publishing Group, 511(7508), p. 216.

Zhou, Y. and Shepherd, J. M. (2010) 'Atlanta's urban heat island under extreme heat conditions and potential mitigation strategies', *Natural Hazards*. Springer, 52(3), pp. 639–668.

Zhu, Z., Wang, S. and Woodcock, C. E. (2015) 'Improvement and expansion of the Fmask algorithm: Cloud, cloud shadow, and snow detection for Landsats 4–7, 8, and Sentinel 2 images', *Remote Sensing of Environment*. Elsevier, 159, pp. 269–277.

View publication stats